Relocation and Comparison of the 2010 M4.1 and 2011 M5.6 Earthquake Sequences in Lincoln County, Oklahoma

Chris Toth[1], Austin Holland[2], Katie Keranen[1], Amie Gibson[2]

[1] University of Oklahoma, Norman, Oklahoma, christopher.toth@ou.edu; [2] Oklahoma Geological Survey, Norman, Oklahoma

Abstract

On February 27, 2010 a M4.1 earthquake occurred in southeastern Lincoln County. 111 aftershocks of this earthquake were recorded through August 2011. At the start of the sequence, the seismic network consisted of six Oklahoma Geological Survey seismic monitoring sites distributed across the state, IRIS Transportable Array coverage on the western half of the state, and NetQuakes instruments ~40 km to the west. Over the remainder of 2010, the coverage of the Transportable Array gradually expanded to include the whole state of Oklahoma. Consequently, part of the 2010 M4.1 aftershock sequence had poor station coverage, particularly at the beginning of the sequence, and events could not be precisely located. On Nov. 6, 2011, a M5.6 occurred in the same region. Aftershocks of this event have been well-recorded with a dense network of temporary local, OGS, and TA stations. Using VELEST, we inverted for a 1-D velocity profile using the P and S-phase picks for 212 earthquakes from the well-resolved 2011 M5.6 earthquake sequence. Sonic logs from nearby wells were used as a priori information to constrain velocity inversion. The well-located M5.6 2011 sequence and the M4.1 2010 sequence were located together using HypoDD. The earthquake locations and associated uncertainties for the 2010 M4.1 earthquake sequence improved dramatically through joint location. The relocated earthquakes for the M4.1 2010 sequence occurred in approximately the same location and delineate a zone with the same orientation as the larger Nov. 2011 earthquake sequence.

Map of Wells and Seismometers

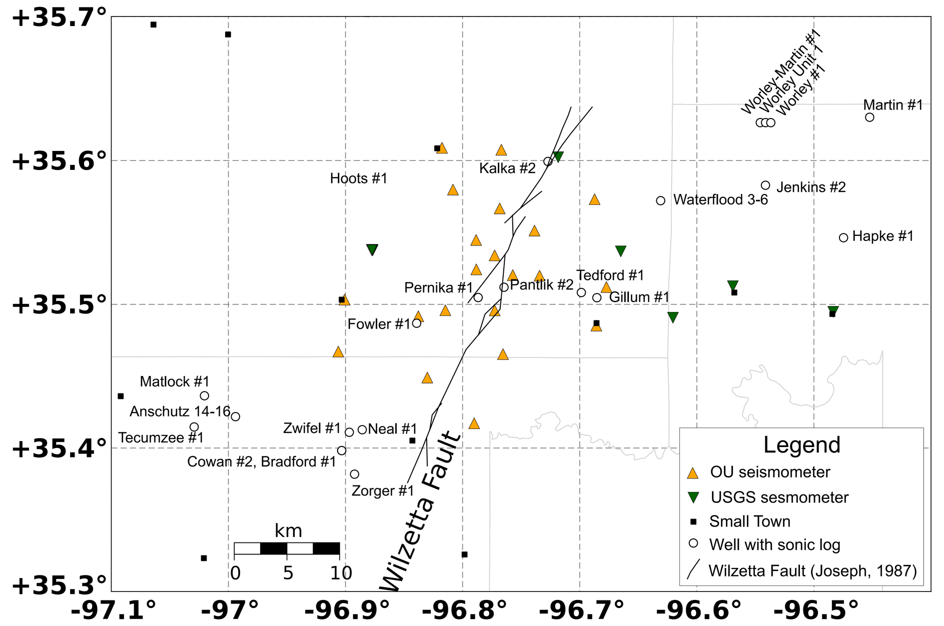

Above: Map of the seismic stations and wells of the region
Below: Map of start and end dates of EarthScope Transportable Array and Regional Seismic Network stations

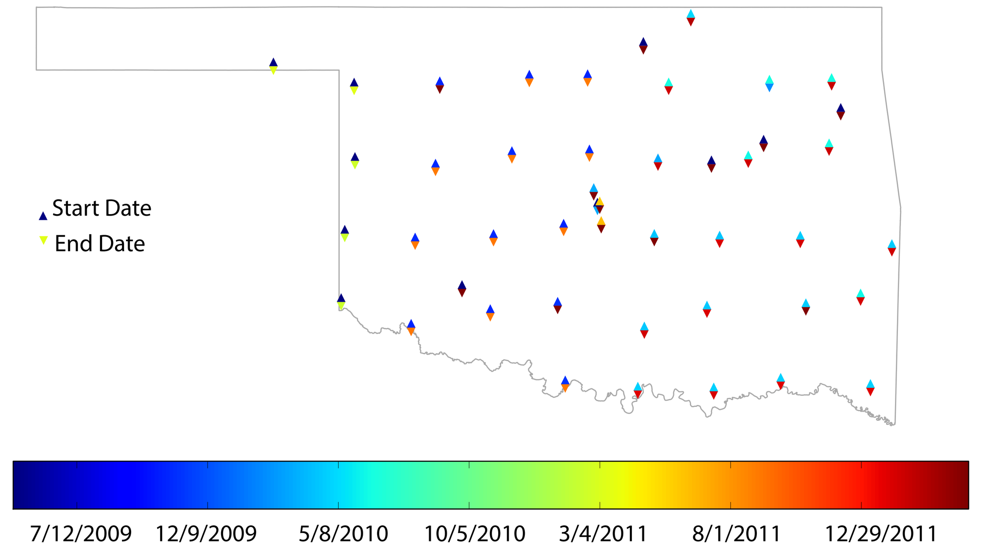

Velocity Analysis

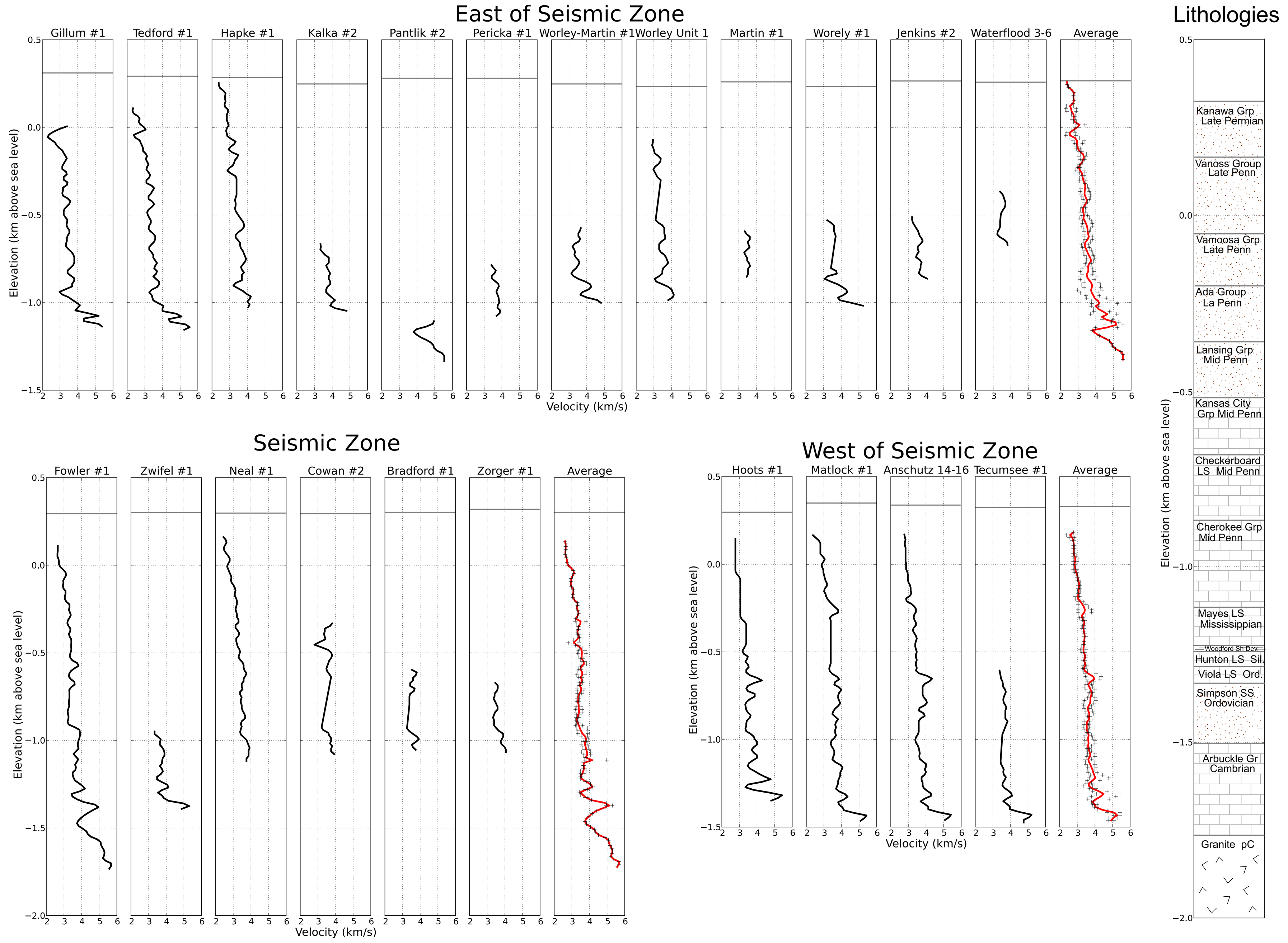

Above: 22 p-wave sonic logs from the immediate area surrounding the earthquake sequences were analyzed. The logs were divided into 3 groups, those east, west, and inside the zone of seismicity. The logs within each group were averaged, and each of the three resulting velocity profiles were used as input models for velocity inversion using VELEST (Kissling et al, 1994). The deepest portion of some of the logs shows alternating high and low velocity layers; since these layers were much thinner than the wavelengths of interest, they were averaged together to simplify the final model. The shallow velocity model derived from the western sonic logs had the lowest inversion residual for stations <40km from the fault zone. Inversion for deeper layers, keeping the shallow velocity profile constant, was then performed in VELEST for all stations <200km from the fault zone. The p-wave and S-wave velocity models were inverted for separately. The final p-wave velocity model yeilded an average station correction of .39s with a standard deviation of .70s, and a final RMS of .064. The s-wave velocity model had an average station correction of .34s with a standard deviation of .72s, and the RMS was .14. Elevations at the wells are represented as a gray line about 0.3 km above sea level.

P- and S- Velocity Models

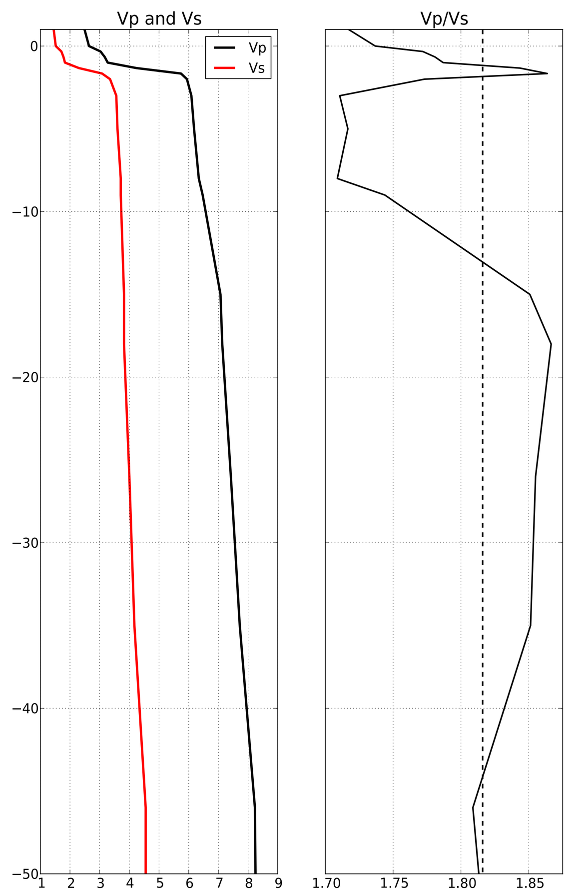

Right: A Vp/Vs ratio was calculated for each layer and a weighted average based on layer thickness was determined to be 1.816.
This average, which was used in the HypoDD relocation (Waldhausser and Ellsworth, 2000), is represented on the graph as a dashed vertical line.

Double-Difference Relocation

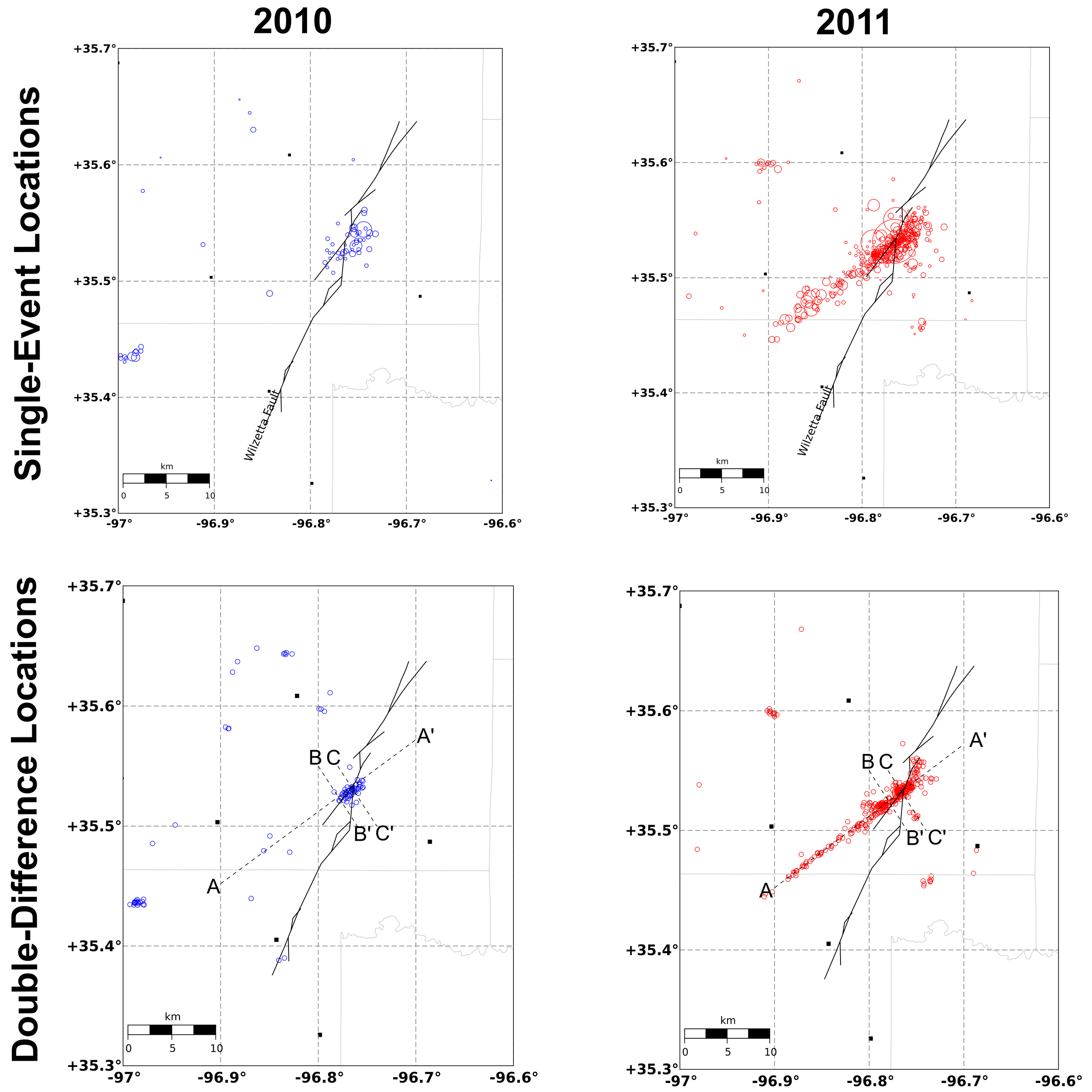

Above: Maps of the earthquake distributions. The left two plots are of the 2010 M4.1 sequence and the right plots are of the 2011 M5.6 sequence. The two upper plots are the single-event locations determined with Seisan and scaled by magnitude. The lower plots are the HypoDD relocated earthquakes. The initial mean event residual for the largest cluster was .063s. After 16 HypoDD iterations, this residual was reduced to .0015s. An examination of the northeast and southwest ends of the cluster of earthquakes shows that the fault may bifurcate in multiple locations. The blue/red color scheme is maintained in subsequent figures. Wilzetta Fault geometry from Joseph (1987).

Below: Subsurface cross-sections of the earthquake distribution. Line A-A' runs along the trend of the sequences. Lines B-B' and C-C' run perpendicular to the sequence, showing a steep north-westerly dip of the fault zone. The southwest portion of A-A' illustrates a linear fault plane and shallow rupture, but the northeast segment has shallow and deep ruptures and a more complex fault zone. Earthquakes occuring within +/- 1km of the cross-section line were included in the projection.

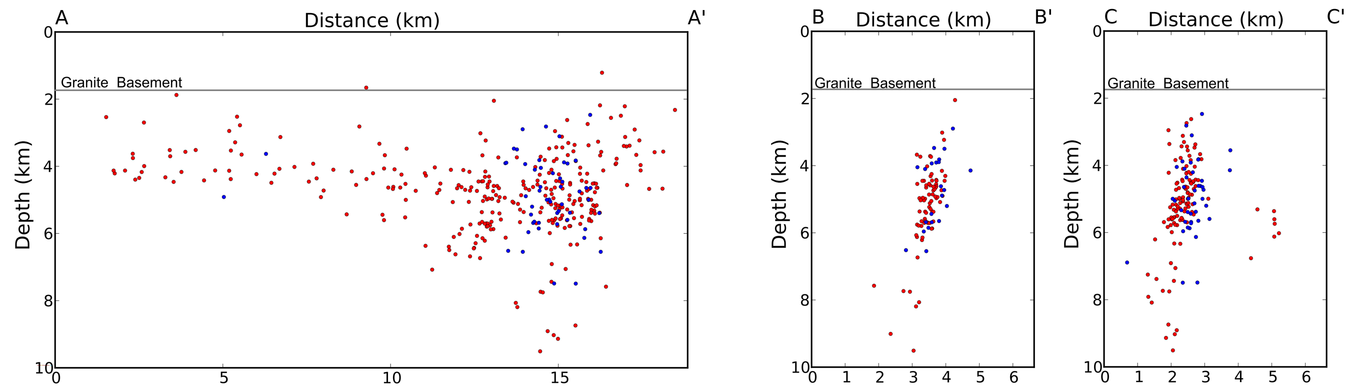

Focal Mechanisms

Right: Locations of relocated earthquakes, scaled by magnitude. Focal mechanisms for the largest event of the 2010 sequence (blue) and for the three largest events of the 2011 sequence (red) are plotted. Most of the focal mechanisms across both sequences are right-lateral strike-slip. The 2011-11-08 Mw4.7 event, shown, was left-lateral strike-slip. Focal mechanisms are generally consistent with the observed seismicity pattern and nearby vertical strike-slip faults. The mapped fault (Joseph, 1987) at the base of the Pennsylvanian and the seismicity within the Precambrian basement both suggest that there is complexity within the Wilzetta Fault system near the epicenter of the largest earthquakes in both the 2010 and 2011 earthquakes. Focal Mechanisms from USGS/SLU.

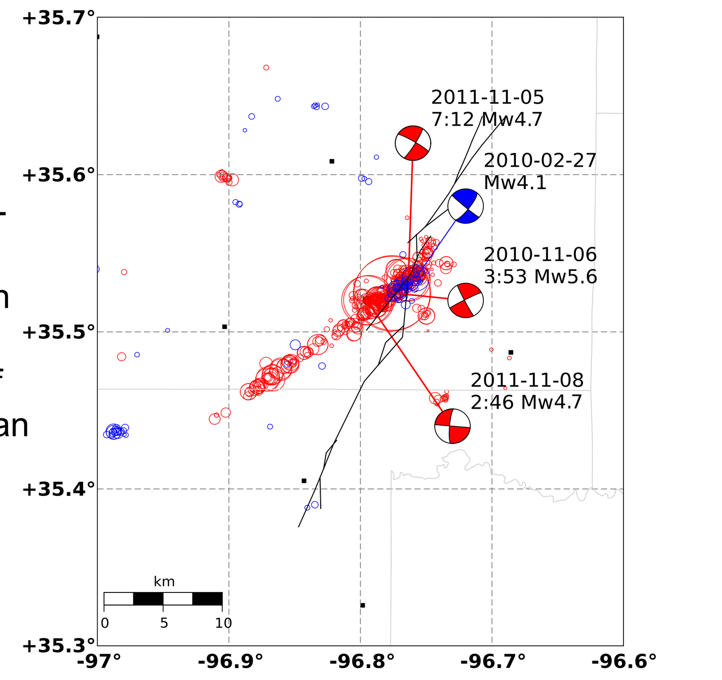

Sequence Timing

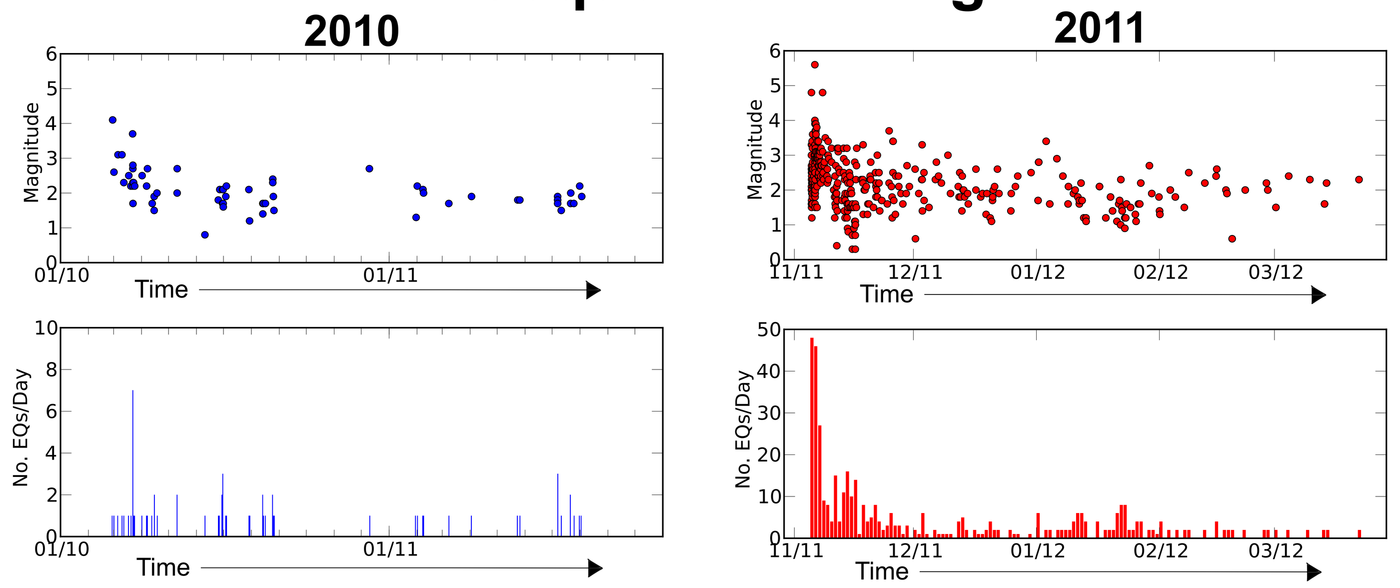

Above: Magnitude vs. Time, and Number of Daily Earthquakes vs. Time plots.

Conclusions and Further Work

-Relocated earthquakes strongly delineate a fault zone striking S55W with a steep north-westerly dip, and both sequences appear to have occured on the same structure.
-Focal motions for the 2010 and 2011 earthquake sequences are high-angle strike-slip faults.
-The main S55W striking fault consistently exhibits right-lateral strike-slip, but the fault appears to bifurcate in at least two locations where different focal mechanisms are observed.
-The 2011 earthquake sequence shows an aftershock decay consistent with Omori's Law. The preceding 2010 sequence, while representing an increase from background seismicity, does not follow Omori's Law.
-The vast majority of ruptures occured in the Precambrian granitic basement.
-Additional data from temporary OU and PASSCAL RAMP stations, which can help elucidate the complexity of the Wilzetta Fault system, will be presented by Katie Keranen Wednesday at 3:30
-In related efforts, a seismic profile through central Oklahoma which uses earthquakes as a source has been conducted. The results of this work will help to further refine the velocity model and perhaps provide a greater understanding of the basement structure in the area.

References

Waldhauser, F. and W.L. Ellsworth, 2000, A double-difference earthquake location algorithm: Method and application to the northern Hayward fault, Bull. Seismol. Soc. Am., 90, 1353-1368.
USGS/SLU Moment Tensor Solutions for North America, http://www.eas.slu.edu/eqc/eqc_mt/MECH.NA/index.html.
Joseph, L., 1987, Subsurface Analysis, “Cherokee” Group (Des Monesian), Portions of Lincoln, Pottawatomie, Seminole, and Okfuskee Counties, Oklahoma, Oklahoma City Geological Society Shale Shaker, December 1986/January 1987.
E. Kissling, W. Ellsworth, D. Eberhart-Phillips, and U. Kradolfer, Initial reference models in local earthquake tomography, J. Geophys. Res., 99, B10, doi:10.1029/93JB03138, 1994